Evaluating DEM conditioning techniques, elevation source data, and grid resolution for field-scale hydrological parameter extraction

Kathryn Woodrow[1,2], John B. Lindsay[1*], Aaron A. Berg[1]

1. Department of Geography, University of Guelph, 50 Stone Road East, Guelph, ON, Canada, N1G 2W1

2. Present address: GEO Morphix Ltd., 348 Bronte Street South, Milton, ON, Canada, L9T 5B6

* Corresponding Author: E-mail: jlindsay@uogueph.ca, Phone: 519-824-4120 ext. 56074

ABSTRACT

Although digital elevation models (DEMs) prove useful for a number of hydrological applications, they are often the end result of numerous processing steps that each contains uncertainty. These uncertainties have the potential to greatly influence DEM quality and to further propagate to DEM-derived attributes including derived surface and near-surface drainage patterns. This research examines the impacts of DEM grid resolution, elevation source data, and conditioning techniques on the spatial and statistical distribution of field-scale hydrological attributes for a 12,000 ha watershed of an agricultural area within southwestern Ontario, Canada. Three conditioning techniques, including depression filling (DF), depression breaching (DB), and stream burning (SB), were examined. The catchments draining to each boundary of 7933 agricultural fields were delineated using the surface drainage patterns modeled from LiDAR data, interpolated to a 1 m, 5 m, and 10 m resolution DEMs, and from a 10 m resolution photogrammetric DEM. The results showed that variation in DEM grid resolution resulted in significant differences in the spatial and statistical distributions of contributing areas and the distributions of downslope flowpath length. Degrading the grid resolution of the LiDAR data from 1 m to 10 m resulted in a disagreement in mapped contributing areas of between 29.4% and 37.3% of the study area, depending on the DEM conditioning technique. The disagreements among the field-scale contributing areas mapped from the 10 m LiDAR DEM and photogrammetric DEM were large, with nearly half of the study area draining to alternate field boundaries. Differences in derived contributing areas and flowpaths among various conditioning techniques increased substantially at finer grid resolutions, with the largest disagreement among mapped contributing areas occurring between the 1 m resolution DB DEM and the SB DEM (37% disagreement) and the DB-DF comparison (36.5% disagreement in mapped areas). These results demonstrate that the decision to use one DEM conditioning technique over another, and the constraints of available DEM data resolution and source, can greatly impact the modeled surface drainage patterns at the scale of individual fields. This work has significance for applications that attempt to optimize best-management practices (BMPs) for reducing soil erosion and runoff contamination within agricultural watersheds.

Keywords: digital elevation models; flowpath enforcement; LiDAR; topographic depressions; spatial resolution.

Highlights

1. Within-field catchments were mapped from LiDAR and photogrammetric DEMs.

2. Varying resolution and source resulted in large differences in drainage patterns.
3. Conditioning methods affected drainage patterns the greatest at fine resolutions.
4. This affects BMP optimizations that rely on accurate field-scale drainage mapping.

1 INTRODUCTION

Topography is a major control of earth surface processes (Jenson, 1991; Florinsky, 1998). In particular, hillslope morphology directly influences surface and subsurface water flow due to the gravitational potential involved in flow path determination (Dunne and Black, 1970; Quinn et al., 1991; Beven and Wood, 1983). Understanding watershed hydrology therefore involves significant knowledge of the land surface. Topography can be used to develop more physically realistic models of hydrological processes due to the inherent relationship between surface relief and downstream flow.

Digital elevation models (DEMs) have contributed substantially to progress in spatial hydrological modelling over the past several decades. DEMs are commonly used to portray earth surface topography and are useful for a number of common hydrological applications such as watershed delineation (Jenson and Domingue, 1988; Jenson, 1991), stream network extraction (O'Callaghan and Mark, 1984, Tarboton, 1997), and surface and near-surface flowpath mapping (Erskine et al., 2006; Costa-Cabral and Burges, 1994). Advanced techniques in elevation data acquisition, DEM interpolation, and hydrological DEM conditioning have revolutionized DEM accuracy and the extraction of topographic derivatives from the digital terrain surface.

Advancements in automated DEM analysis techniques have allowed researchers to transfer derived DEM surface parameters into meaningful inputs for hydrological models (Jenson and Domingue, 1988; Martz and Garbrecht, 1998). Automated hydrological parameterization methods ultimately rely on two critical factors: 1) a method for overland flow routing to define contributing areas and channel networks (O'Callaghan and Mark, 1984), and 2) a method for managing topographic depressions and flat areas that inhibit overland flow routing (Martz and Garbrecht, 1998; Martz and Garbrecht, 1999).

Flow paths in DEMs are created based on elevation differences among grid cells and their downslope neighboring cells. Flow routing algorithms use DEMs to estimate the direction of the downslope redistribution of topographically driven overland flow passing through each grid cell in the DEM (Tribe, 1992). The flow direction information derived from these routing algorithms can be used to derive hydrological attributes such as upslope catchment area and the location of drainage divides. Each flow routing method has a unique approach redistributing flow from a grid cell to its downslope neighbours. Algorithms such as the D8 (O'Callaghan and Mark, 1984) and D-infinity (Tarboton, 1997) have been incorporated into hydrological models as methods for overland flow routing prior to watershed parameterization.

Topographic depressions, often termed sinks or pits (Lindsay, 2016a), are characteristically prevalent in DEMs. Depressions can be defined as an individual DEM grid cell or groups of neighbouring grid cells that do not have a downslope flow outlet (Jenson and Domingue, 1988). Surrounding grid cells possess higher elevation values resulting in a topographic hollow or bowl-like feature. DEM depressions are particularly problematic for overland flow routing because they accumulate water, creating discontinuity in flow paths and negatively influencing the modelled hydrological response of a catchment (Lindsay and Creed, 2005; Grimaldi et al., 2007). DEM conditioning techniques have been developed to resolve the negative effects associated with topographic depressions. Each conditioning technique is based on an assumption regarding the true nature of depressions. Topographic depressions are actually a combination of artifact and actual features (Lindsay

and Creed, 2006; Grimaldi et al., 2007). Artifact depressions typically result from elevation data inaccuracy, interpolation error, and limited data resolution (Walker and Willgoose, 1999). Actual depressions, however, represent true topographic features on the landscape (Lindsay and Creed, 2005). Though less common than artifact depressions, real depressions exist in most non-fluvial landscape, including glacial and karst landscapes.

Hydrological DEM conditioning techniques are distinguished by their approach for accommodating depression features. Every technique is designed to enforce downstream flow by connecting flow path grid cells. DF (e.g. Jenson and Domingue, 1988; Planchon and Darboux, 2001; Wang and Liu, 2006), DB (e.g. Rieger, 1998; Lindsay and Dhun, 2015), and SB (e.g. Saunders, 1999) are the most common types of drainage enforcement or conditioning methods. DF techniques remove depression features by raising the elevation value of a depression cell. DB, however, works to lower the grid cells that are adjacent to depression cells (Rieger, 1998; Lindsay, 2016a). SB uses digital streamline data to reinforce mapped drainage networks in a DEM (Hutchinson, 1989; Saunders, 1999; Lindsay, 2016b). Elevation values in a DEM along a mapped stream network are lowered, or 'burned' into the elevation model (Saunders, 1999). While SB is effective at removing depressions situated along the mapped stream line, the technique cannot remove depressions in hillslope positions within the DEMs and must therefore be followed by a DF or DB operation to ensure continuous flowpaths.

Traditional flow enforcement methods can each resolve flowpath interruptions resulting from DEM depressions; however, the effectiveness of these techniques in human-modified landscapes has been limited. Lindsay and Dhun (2015) developed a novel DB technique to accommodate the linear flow paths associated with anthropogenic landscapes, such as agricultural drainage ditches. The construction of various landscape infrastructure has been shown to increase downstream water discharge and modify surface drainage networks (Duke et al., 2003). The sensitivity of DEM-derived drainage patterns to varying flow enforcement methods is particularly relevant in human-modified, agricultural basins, which are often the focus of intensive water quantity and quality modelling applications. Furthermore, the characteristic low-relief topography of many agricultural landscapes has the potential to demonstrate substantial sensitivity to the specific flow enforcement technique used to condition DEMs. Previous research has demonstrated that modeled surface hydrological attributes are sensitive to DEM grid resolution and elevation source data across a range of topographic settings and landscape types (Chang and Tsai, 1991; Wolock and Price, 1994; Gao, 1997; Wolock and McCabe, 2000; Deng, Wilson, and Bauer 2007; Sørensen and Seibert, 2007; Wu, Li, and Huang, 2008). However, there has been less focus on the hydrological implication of DEM conditioning techniques particularly over low relief agricultural areas.

The purpose of this study is to examine and evaluate the effects of various DEM grid resolutions, elevation source data, and conditioning techniques (i.e. depression removal and flow enforcement methods) on field-scale hydrological parameter extraction and distribution. This study aims to assess the uncertainty associated with various DEM characteristics. In this case, uncertainty refers to data precision, or the degree to which derived hydrological parameters vary when grid resolution, source data, and conditioning technique is changed. We therefore ask, how does DEM grid resolution, elevation source data, and DEM conditioning techniques influence the definition of field-scale drainage divides and their downslope flowpath length patterns? While many different DEM-derived topographic attributes are used in hydrological applications (e.g. the topographic wetness index), surface drainage patterns are characterized by the locations of divides and the timing of surface and near-surface flow is related to the distribution of flowpath lengths within individual catchments.

2 DATA AND METHODOLOGY

2.1 Study Area

The study was conducted using elevation data acquired from the Rondeau Basin (42°17'N 81°52'W), a Lake Erie coastal zone in Kent County, southwestern Ontario, Canada (Figure 1). This site was chosen because of its size, the availability of data (particularly LiDAR data), and because it is representative of the regional topography. The topography of the study area is typical of agricultural landscapes within the larger Great Lakes region. The northeastern portion of the basin runs east to west along the Blenheim moraine, resulting in gently undulating topography towards the centre of the basin and gently sloping topography leading away from the moraine. Deep gullies drain the northern portion of the watershed, with flow reaching the thirteen main tributaries that drain south to Lake Erie (Gilbert and Locke, 2007). These features constitute a portion of the approximately 12,000 ha Rondeau watershed. The dominant land use in the region is agriculture. Intensive farming practices produce increased agricultural runoff, exacerbating high nutrient and sediment loading from local fields to adjacent draining tributaries (e.g. Molder et al. 2015).

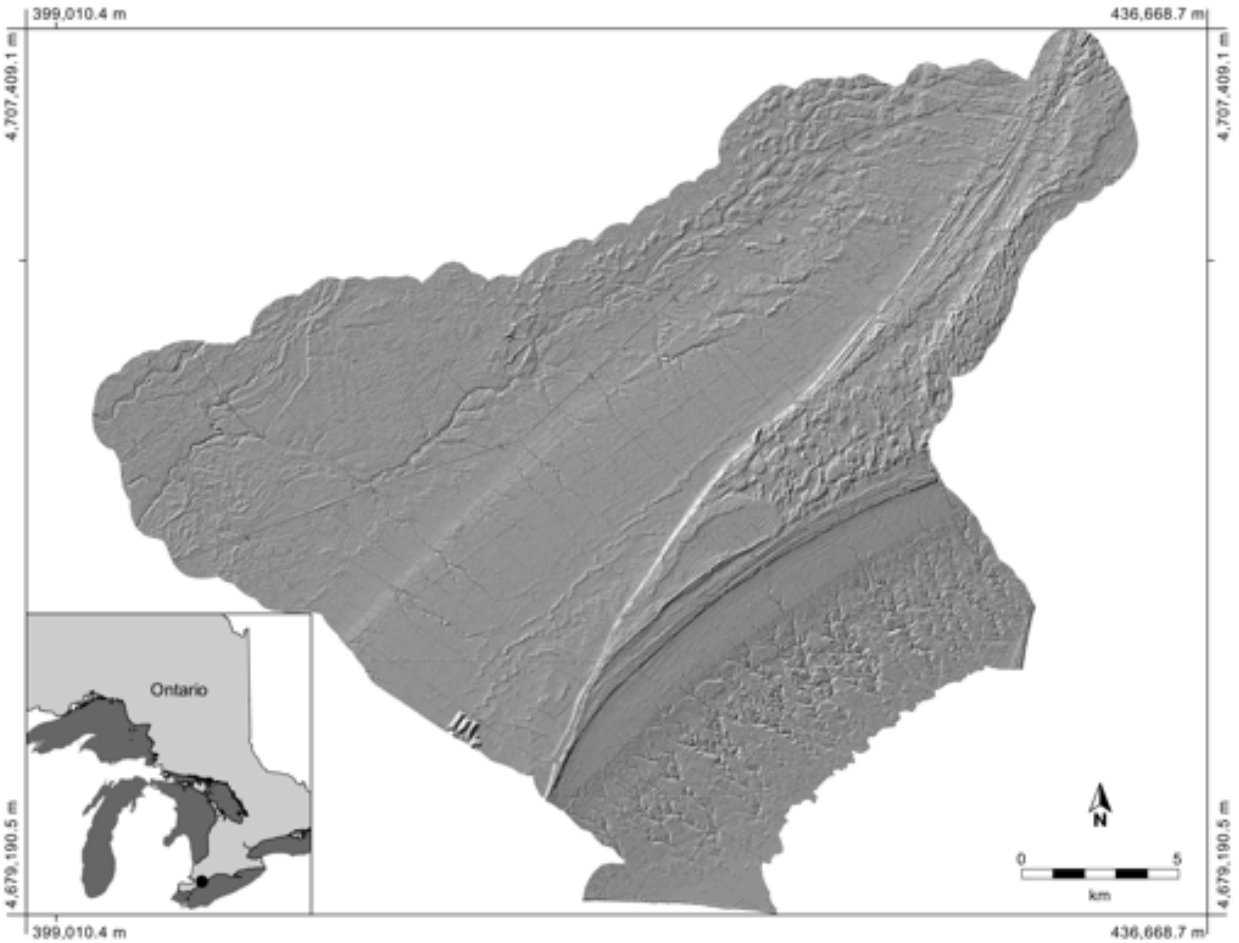

Figure 1: Hillshade image of Rondeau Watershed study area in Southwestern Ontario.

2.2 Data

A publicly accessible DEM was collected for the study area: the 2006 Ontario Provincial Tiled DEM Dataset, produced by the Ontario Ministry of Natural Resources (OMNR) at a 10 m grid resolution. This DEM was developed using past contour elevation data, specific spot height elevation data derived from the 2010 Southwestern Ontario Orthophotography Project (SWOOP) data set, and the Ontario Hydro Network (OHN) stream network

data set. The stated vertical and horizontal accuracies of the SWOOP elevation data product is 0.50 m. LiDAR data over the study area were acquired over a two-day period (May 4th/5th) in the spring of 2008. Raw point cloud LiDAR data were obtained from the Ontario Ministry of Agriculture and Food (OMAF) in LAS file format. The raw LiDAR point cloud was collected with a target vertical accuracy of at least 0.15 m. The point cloud was used to interpolate three LiDAR DEMs at 1 m, 5 m, and 10 m resolutions using an inverse-distance-weighted (IDW) scheme. Whitebox GAT's (Lindsay, 2014) IDW LiDAR interpolation technique was used and incorporated all last-return points from the data set. Whitebox GAT's LiDAR Off Terrain Objects (OTO) removal tool was also used to eliminate data points associated with buildings. The conditioning techniques used for this dataset are described in the following sections.

The OHN stream data was used as ancillary data for the stream burning drainage enforcement technique outlined below. The Agricultural Resource Inventory (ARI) dataset was used to outline agricultural field boundaries and non-agricultural land cover (e.g. urban, forest, homestead). The 2013 ARI field polygon dataset for Kent County was obtained from OMAF. ARI field polygons were used to create and derive individual raster field boundaries to be used as flow outlet cells for field-scale upslope contributing area delineation. In total, the site contained 7933 individual fields.

2.3 DEM Conditioning

The impacts of three common conditioning techniques were examined on each interpolated DEM. These techniques included: 1) DF (Wang and Liu, 2006), 2) DB (Lindsay and Dhun, 2015), and 3) SB (Saunders, 1999). The SB method used DF as a post-processing method to remove all remaining depressions.

Each technique was used to create different hydrologically corrected DEMs for each DEM dataset. Each of these three DEM conditioning techniques have been implemented as plugin tools within the open-source GIS Whitebox GAT (Lindsay, 2014). The DB algorithm (Lindsay and Dhun, 2015) modified the elevations of grid cells along non-straight breach channels connecting pit cells to distant grid cells of lower elevation, with a path dictated by a minimum elevation modification criterion. For SB, the *Burn Streams* tool was used to lower all grid cells in the DEM that were coincident with the mapped stream network by 10 m, with subsequent modifications to ensure monotonically downward flowpaths along the streams. The tool also imposed a gradient along adjacent hillslopes toward the stream cells, which was used to lessen the occurrence of erroneous parallel streams. For this study the impact of the conditioning techniques on the definition of field-scale drainage divides, measured as upslope contributing areas and their downslope flowpath length was assessed over 12 DEMs (4 DEMs × 3 conditioning methods).

Upslope contributing area (UCA) is fundamental in hydrological models, as it represents the area that can potentially produce overland flow to a location of interest (Tarboton et al., 1991; Quinn et al., 1991). For this study UCA was determined for each DEM to evaluate the impact of grid resolution, data source, and conditioning method. The D8 flow direction algorithm (O'Callaghan and Mark, 1984) was used to assign flow directions to all DEM grid cells. Individual ARI raster field boundaries were used as the various target cells or 'outlets' for field-scale flow accumulation. A simple boundary tool was used to identify field-scale contributing areas for all field edges, producing multiple sub-basins for each field. The spatial impact of resolution, data, and conditioning was defined as the percent area in disagreement among field-scale contributing areas derived from DEMs with differing hydrological conditioning techniques, source data, and resolutions.

Downslope flowpath lengths (DFL) were derived for field contributing areas in each DEM using the D8 flow algorithm to assess the impact of resolution, data, and conditioning on statistical distributions of DEM-derived parameters. DFL is an important variable in hydrological analysis because it reflects distance to a catchment

outlet along an overland flowpath; this is particularly significant for understanding the timing of flow to a specific outlet (Liu et al., 2003). DFL was derived for the field-scale UCAs delineated for all DEMs.

2.4 Statistical Analysis

Kolmogorov-Smirnov (K-S) two-sample tests were used to evaluate whether resolution, data, or conditioning technique significantly affected the statistical distribution of DFL distributions between various DEMs. The K-S test is a non-parametric test that determines whether the maximum difference (D_{max}) between the cumulative probability distributions of two samples is greater than expected (Norcliffe, 1982). K-S tests are also sensitive to differences in both sample distribution location and shape, which is particularly important for assessing the effects of conditioning techniques. Depression removal affects distribution tails because pits commonly occur in areas of lower elevation (Rieger, 1998). Note that while alternative goodness-of-fit tests, such as the Cramér-von Mises and the Anderson-Darling tests, could have been used for these analyses, the K-S goodness-of-fit test was chosen because it was implemented within the GIS software used for this study.

A total of 36 K-S tests (three tests per DEM) were conducted to assess grid resolution, data source, and DEM conditioning methods. Tests were performed on random samples of grid cells throughout each DEM. Sample size in each case reflected approximately 0.02% of the total number of grid cells in each DEM (10 m DEMs, n = 1,500; 5 m DEM, n = 7,800; 1 m DEM, n = 189,000).

3 RESULTS

3.1 Assessment of UCA

The percentage of total field contributing areas in disagreement among the 10 m, 5 m, and 1 m DEMs are displayed in Figure 2. The DF scenarios for all three DEM resolution comparisons produced the highest percentage of UCA in disagreement. For example, the filled 10 m and 1 m DEM comparison yielded 37.3% disagreement, while the remaining 10 m and 1 m comparisons showed 29.9% and 29.4% for DB and SB respectively. Disagreement was higher for all 10 m and 1 m comparisons than any of the 5 m to 1 m comparisons. Total field contributing area in disagreement between the 10 m provincial DEM and the 10 m LiDAR DEM is shown in Figure 3. The area of disagreement between each DEM ranged from 39.9% for the SB DEM comparison to 47.5% for the DF comparison and 46.9% for the DB DEMs.

The percentage of total field contributing areas in disagreement among various conditioned DEMs at various spatial resolutions is displayed in Figure 4. The DF and DB comparisons range from 12.9% to 36.5% total disagreement; DF and SB from 14.3% to 31.2%; and SB and DB from 15.2% to 37%. Highest disagreement in UCA for each individual DEM is evident in burned and breached comparisons. The lowest percentages of UCA disagreement occur in the 10 m provincial DEM comparisons. In every scenario, the area of disagreement almost doubles when the 1 m LiDAR is used for comparison, with the 10 m LiDAR and 5 m LiDAR typically falling midway between the minimum and maximum UCA in disagreement.

3.2 Assessment of DFL

Table 1 shows the results of K-S tests comparing the field-scale DFL distributions derived from pairs of LiDAR DEMs of varying resolution, specifically comparing the 1 m and 5 m resolution DEMs, the 5 m and 10 m DEMs, and the 1 m and 10 m DEMs. Each comparison yielded highly statistically significant differences ($p < 0.001$) between the modeled DFL distributions. It is apparent from these results that DFL is particularly sensitive to DEM grid resolution.

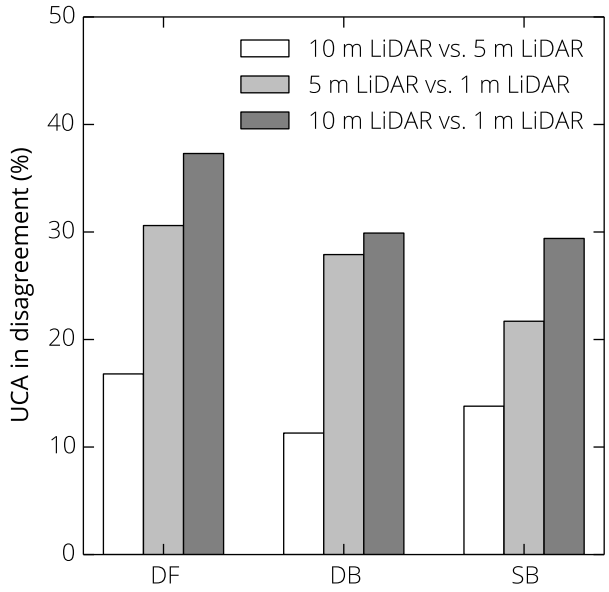

Figure 2: Spatial differences in field derived UCA between 10 m and 5 m LiDAR DEMs, 5 m and 1 m LiDAR DEMs, and 10 m and 1 m LiDAR DEMs (varying resolution) as indicated by % area in disagreement.

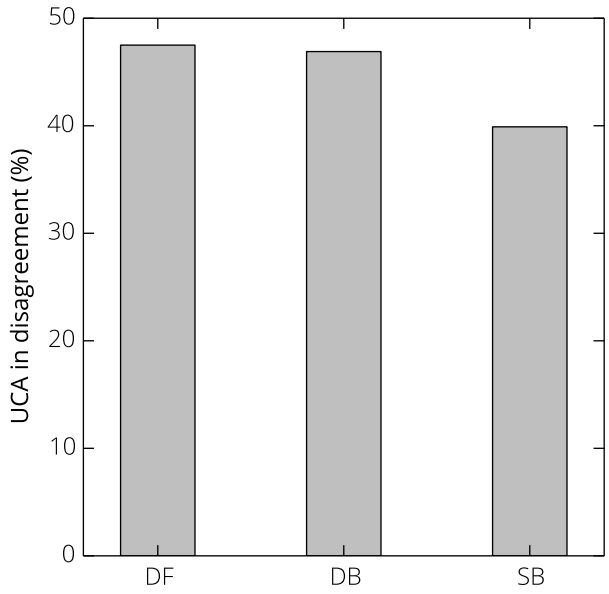

Figure 3: Spatial differences in field derived UCA between 10 m Provincial DEM and 10 m LiDAR DEM (varying elevation data source) as indicated by % area in disagreement.

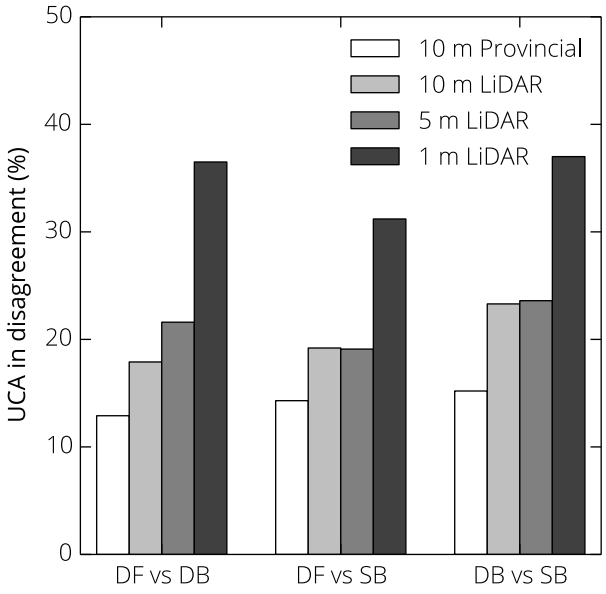

Figure 4: Spatial differences in field derived UCA between various DEM conditioning techniques as indicated by % area in disagreement.

Table 1: K-S tests for statistically significant differences in field derived DFL distributions between 1 m and 10 m, 5m and 10m, 1m and 5m LiDAR DEMs, respectively.

	1 m LIDAR DEM : 10 m LIDAR DEM	**5 m LIDAR DEM : 10 m LIDAR DEM**	**1 m LIDAR DEM : 5 m LIDAR DEM**
DF	$D_{max} = 0.188$	$D_{max} = 0.137$	$D_{max} = 0.160$
	$p < 0.001$	$p < 0.001$	$p < 0.001$
DB	$D_{max} = 0.260$	$D_{max} = 0.165$	$D_{max} = 0.276$
	$p < 0.001$	$p < 0.001$	$p < 0.001$
SB	$D_{max} = 0.157$	$D_{max} = 0.291$	$D_{max} = 0.208$
	$p < 0.001$	$p < 0.001$	$p < 0.001$

The DFLs derived from the 10 m provincial and 10 m LiDAR DEMs were compared for each conditioning technique to highlight significant differences as a result of varying source data (Table 2). Testing showed significant differences in DFL distributions among the DF ($p = 0.014$) and DB ($p = 0.002$) DEM pairs. The DFL distributions derived from the SB Provincial DEM were also found to be significantly different than the DF ($p = 0.022$) and DB ($p = 0.049$) 10 m LiDAR DEMs.

Table 2: Comparison of differences in the cumulative DFL distributions derived using the three DEM conditioning techniques and DEM data source.

		10 m LiDAR DEM		
		DF	**DB**	**SB**
10 m Provincial DEM	**DF**	$D_{max} = 0.092$ $p = 0.014$	$D_{max} = 0.042$ $p = 0.682$	$D_{max} = 0.048$ $p = 0.509$
	DB	$D_{max} = 0.014$ $p = 1.000$	$D_{max} = 0.108$ $p = 0.002$	$D_{max} = 0.041$ $p = 0.678$
	SB	$D_{max} = 0.091$ $p = 0.022$	$D_{max} = 0.079$ $p = 0.049$	$D_{max} = 0.065$ $p = 0.174$

Table 3: Results of K-S tests used to evaluate statistically significant differences in DFL distributions between three conditioned 1 m LiDAR DEMs and three conditioned 5 m LiDAR DEMs.

Conditioning Methods	**1 m LiDAR DEM**	**5 m LiDAR DEM**
DF vs. DB	$D_{max} = 0.122$ ($p < 0.001$)	$D_{max} = 0.042$ ($p = 0.004$)
DF vs. SB	$D_{max} = 0.152$ ($p < 0.001$)	$D_{max} = 0.017$ ($p = 0.638$)
DB vs. SB	$D_{max} = 0.056$ ($p = 0.132$)	$D_{max} = 0.0390$ ($p = 0.007$)

Table 3 compares the effects of altering DEM conditioning methods on the derived distributions of DFL. The DFL distributions derived from were found to be statistically different for the DF and DB DEMs, both at the 1 m ($p < 0.001$) and 5 m ($p = 0.004$) grid resolutions. At the 1 m resolution, significant differences ($p < 0.001$) were also found in the DFL distributions derived from the DF and SB DEMs. Breaching and stream burning yielded statistically similar DFL distributions at both tested resolutions (Table 3). The differences among the comparisons of conditioning methods were all more pronounced at the finer 1 m resolution than they were at the 5 m grid resolution.

4 DISCUSSION

4.1 Spatial and Statistical Differences Associated with Various DEM Grid Resolutions

The effects of DEM grid resolution on subsequent hydrological parameter extraction have been widely investigated. Kienzle (2004) found that upslope contributing area identification depends strongly on DEM resolution. The results of the present study confirm the results of Kienzle (2004) indicating that approximately 30-37% of total derived field-scale UCAs were in disagreement for all 10 m and 1 m LiDAR DEM comparisons, regardless of conditioning technique. The 10 m and 5 m DEM comparisons ranged from 11-17%, while the disagreement observed based on the 5 m and 1 m comparisons were between 22% and 30%. Simulations that included the 1 m LiDAR DEM as a comparison produced greater differences in derived UCA, demonstrating the effect of finer resolution data on spatial hydrological modelling. Figure 5 shows a field in the Rondeau watershed following UCA delineation in the 10 m LiDAR DEM and 1 m LiDAR DEM. The 1 m DEM delineates four contributing areas to individual field boundaries, whereas the 10 m DEM delineates two larger, more generalized, contributing areas for the same field. The two remaining sub-basins draining to the west and

south field edges are severely truncated in the 10 m DEM. Studies confirm that decreased DEM resolution results in more generalized contributing areas, especially in small catchments (Wolock and Price, 1994; Zhang and Montgomery, 1994; Saulnier et al., 1997). For field-scale analysis, this is even more problematic as the edge of the field from which drainage is expected is uncertain.

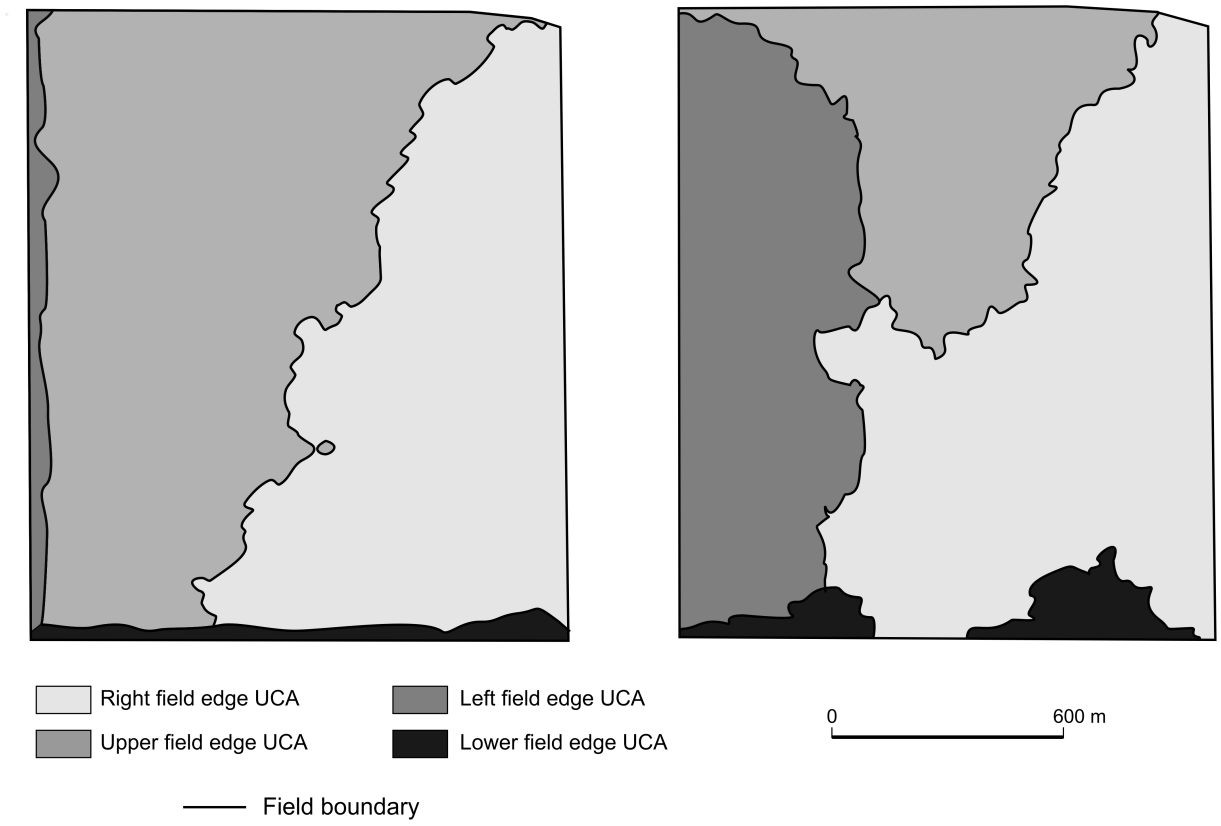

Figure 5: UCA delineation on Rondeau field in 10 m LiDAR DEM (a) and 1 m LiDAR DEM (b); note differences in drainage divides and subsequent derived field sub-basins as a result of DEM resolution.

K-S tests for statistical differences in derived DFL distributions between each DEM produced *p*-values <0.001 for all simulations (Table 1). Significant differences in DEM distributions were evident for all comparisons, indicating that grid resolution is a major factor in the distribution of hydrological parameters. Grid cell size has been shown to significantly affect the cumulative frequency distributions of contributing area, topographic index, and hydrological simulations (Zhang and Montgomery, 1994).

Stream patterns derived from coarse resolution DEMs must rely on large-scale topographic features to develop flow patterns. Finer-resolution DEMs have significantly improved landscape detail to overcome the potential misrepresentation associated with coarse DEM grids. Walker and Willgoose (1999) and Zhang and Montgomery (1994) suggest that a 10 m DEM grid resolution presents the best compromise for simulating hydrological processes at the watershed scale. However, at the hillslope and field scale, fine-resolution LiDAR DEMs are better suited for modelling hydrological processes. The 1 m LiDAR DEM can identify small-scale catchment areas that cannot be modelled by the 10 m DEM due to coarser grid resolution. Many agricultural watersheds have been altered by human-modifications such as drainage ditch construction. The 1 m LiDAR

DEM accommodates many of these features in contributing area identification. Differences in derived UCA and DFL distributions between coarse and fine resolution DEMs are a result of variations in DEM topographic detail.

4.2 Spatial and Statistical Differences Associated with Various DEM Elevation Source Data

DEM accuracy is typically linked to elevation source data. DEM surface derivatives can therefore be sensitive to initial elevation data used in DEM creation. Spatial analysis results demonstrate a range of approximately 40%-47.5% disagreement in derived field UCA between 10 m LiDAR and 10 m provincial DEM comparisons. A similar range of disagreement was present across conditioning techniques, suggesting little sensitivity of the amount disagreement based on conditioning method (Figure 3). The magnitudes of disagreement for DEM source data comparison were larger than the magnitudes examined for grid-resolution comparisons (Figure 2), suggesting that source data, in this case, greatly influenced variations in hydrological attribute derivation.

Statistical differences in DFL distributions among the 10 m provincial and 10 m LiDAR DEM comparisons were significant for only the DF and DB K-S tests (Table 2, diagonal). The spatial differences that resulted from varying source data were also expected during statistical analysis; however, the SB comparison between the 10 m LiDAR and 10 m provincial DEMs was found to be insignificant with a random sample size of 1500 grid cells. This result may be partially expected based on the methods used to develop the provincial DEM. The 10 m provincial DEM was interpolated using the OHN streamline data. Using the OHN as ancillary data for the stream burning analysis of the 10 m LiDAR DEM would have imposed the same streamline source data on both DEMs reducing differences in the distribution of DFLs between the provincial and LiDAR data sets as a result of common drainage network configurations.

Research indicates that DEMs are commonly limited by their original elevation source data (e.g. Walker and Willgoose, 1999; Garbrecht and Martz, 2000; Florinsky, 1998; Zhang et al., 2008). Walker and Willgoose (1999) found that the underlying data source used for deriving DEMs is a major determinant of surface derivatives and a crucial factor in observed differences between those derivatives. Elevation data can significantly vary in terms of data type and data collection. The 10 m provincial DEM was derived from past contour elevation data and specific spot height elevation data. Contour data and spot elevations, however, can be grossly inaccurate (Robinson, 1994; Zhang and Montgomery, 1994). It is likely that variation in DEM source data between the LiDAR and provincial DEMs resulted in subsequent variations in corresponding grid cell elevations contributing to the observed differences in UCAs and DFL distributions.

4.3 Spatial and Statistical Differences Associated with Various DEM Conditioning Techniques

Topographic depressions are ubiquitous in all DEMs as a result of data collection and data interpolation error as well as limited DEM resolution. Conditioning methods that overcome the negative hydrological impacts associated with depressions achieve drainage enforcement in a number of ways. The three conditioning methods assessed in this study showed some significant spatial and statistical differences in derived UCA and DFL. The spatial analysis revealed relatively similar ranges in percent UCA in disagreement between each comparison. DF and DB comparisons for all four DEM scenarios showed a range of approximately 13%-37% (Figure 4). DF versus SB and DB versus SB showed similar UCA disagreement ranging from 14%-31% and 15%-37%, respectively. There was little variation in UCA disagreement between different conditioning for all DEMs. The 10 m provincial DEM had a disagreement range from 13%-15% in all three conditioning comparisons. The 10 m LiDAR and 5 m LiDAR DEMs had similar ranges between 18%-23% and 19%-24% respectively. The 1 m LiDAR DEM comparisons produced a larger range from approximately 31%-37% disagreement. Low variation in conditioning comparisons (Figure 4) for each DEM suggests that conditioning method had less impact on

derived UCA than the spatial resolution of the DEM (as previously discussed). Although, at higher resolutions, lower disagreement percentages were evident when DF and SB were compared, suggesting greater agreement between the two. However it should be noted that, the SB processing methodology also incorporated depression filling to resolve external topographic depressions outside of burned channel networks in the DEM.

The spatial analysis also revealed a significant increase in percent UCA in disagreement for all 1 m LiDAR DEM simulations. This suggests that DEM sensitivity to conditioning technique increases with increasing grid resolution. The effects of depressions on overland flow routing can vary significantly depending on DEM resolution (Lindsay and Creed, 2005). For example, small depressions are readily distinguishable in fine-resolution LiDAR data; however, those depressions are not accounted for in coarser resolutions that generalize topographic features in the landscape (Zhang and Montgomery, 1994). The 1 m LiDAR DEM can readily represent small-scale topographic features that influence overland flow, such as agricultural tillage patterns and road drainage ditches. At finer resolutions, filling techniques remove those features, creating digital ponding that alters natural drainage patterns (Rieger, 1998). Lindsay and Dhun's (2015) breaching technique accommodates the linear flow features in human-modified landscapes. The disagreement in UCA between DF and DB techniques is therefore higher in the 1 m LiDAR DEM comparisons because of its ability to model small-scale topographic variation. The SB technique performed similarly. The OHN streamline data used to 'burn' streams proved highly accurate. Difficulties may arise in SB techniques when streamline data varies from the digitally derived stream network, creating parallel stream effects (Callow et al., 2007).

K-S tests for statistical differences in DFL distributions among DEM simulations reveal contrasting results. Differences between the provincial and LiDAR data sources at the 10 m resolution were significant for the DF and SB comparison and the DB and SB comparison (Table 2). The 5 m LiDAR DEM tests showed significance for the DF and DB comparison and the DB and SB comparison (Table 3). The 1 m LiDAR DEM tests also showed significant differences for two comparisons: DF and DB and DF and SB (p-values <0.001) (Table 3). The two significant 10 m DEM inter-conditioning technique comparisons included the SB method (Table 2). For the two statistically significant 5 m LiDAR DEM simulations, the DB technique was common (Table 3). Significant 1 m LiDAR comparisons included the DF technique (Table 3). Studies have shown that filling techniques have a greater impact on both the spatial and statistical distribution of terrain attributes when compared to breaching techniques (Lindsay and Creed, 2005; Rieger, 1998). These results do not show one particular technique that is responsible for creating statistically significant differences in DFL distributions, adding to the uncertainty associated with optimal DEM conditioning.

5 CONCLUSIONS

Evaluating the effects of DEM grid resolution, elevation source data, and hydrological conditioning techniques on the spatial and statistical distribution of hydrological attributes of an agricultural watershed in Southwestern Ontario indicate the following conclusions:

1. DEM grid resolution directly influences the spatial and statistical distribution of derived hydrological attributes at the field-scale. Coarser resolution DEMs resulted in a mixture of larger and severely truncated field catchments, likely as a result of the inability of coarser scale terrain models to accurately represent within-field low-relief ridges that serve as salient drainage divides. The comparison of DFL distributions among DEMs with various resolutions showed statistically significant differences in all cases; however, the sensitivity in DFL distributions owing to varying grid resolution were more pronounced in DEMs treated with DB and SB flow enforcement methods than with DF.

2. DEM elevation source data directly affects derived hydrological surface derivatives. When compared, the high-density LiDAR data set and the contour-based provincial DEM dataset showed significantly different spatial and statistical distributions of UCA and DFL. All three of the tested DEM conditioning techniques demonstrated some level of sensitivity in DFL distributions due to varying DEM source data.

3. DEM sensitivity to hydrological conditioning techniques increases significantly with DEM grid resolution. Variations in derived hydrological parameters among all conditioning method comparisons increased in the finer resolution LiDAR DEM simulations. The method chosen to hydrologically condition a DEM is highly dependent on the landscape reflected in the DEM and the DEM grid resolution. Therefore, greater consideration of appropriate DEM conditioning methods is required, particularly in research that uses fine-resolution LiDAR DEMs to model hydrological hillslope and field-scale processes within lower relief landscapes.

DEM grid resolution remains a significant determinant of terrain attribute derivation. The use of fine-resolution LiDAR data for advanced hydrological modelling applications is growing in application. Understanding the sensitivity of hydrological terrain attributes to DEM conditioning techniques is important for future flowpath modelling applications. In addition, a greater understanding of the effects of conditioning techniques on accurate surface and near-surface flowpath modelling will be crucial for studies that incorporate fine-resolution LiDAR DEMs.

6 ACKNOWLEDGEMENTS

The authors would like to thank Editor Prof. K. Georgakakos and the anonymous reviewers for their significant contributions to the final manuscript. This work was partially funded through a grants provided by the Ontario Ministry of Agriculture, Food and Rural Affairs (OMAFRA), the Natural Sciences and Engineering Research Council of Canada (NSERC), and the Ontario Research Fund.

7 REFERENCES

Beven, K., and E.F. Wood (1983), Catchment geomorphology and the dynamics of runoff contributing areas, *J. Hydrol.*, 65, 139-158.

Callow, J.N., K.P. Van Niel, and G.S. Boggs (2007), How does modifying a DEM to reflect known hydrology affect subsequent terrain analysis? *J. Hydrology*, 332, 30-39.

Chang, K.T. and B.W. Tsai, 1991. The effect of DEM resolution on slope and aspect mapping, *Cartography and Geographic Information Systems*, 18(1), 69-77.

Costa-Cabral, M.C., and S.J. Burges (1994), Digital elevation model networks (DEMON): a model of flow over hillslopes for computation of contributing and dispersal areas, *Water Resour. Res.*, 30(6), 1681-1692.

Deng, Y., Wilson, J.P. and B.O. Bauer, 2007. DEM resolution dependencies of terrain attributes across a landscape, *International Journal of Geographical Information Science*, 21(2), 187-213.

Duke, G.D., S.W. Kienzle, D.L. Johnson, and J.M. Byrne (2003), Improving overland flow routing by incorporating ancillary road data into digital elevation models, *J. Spatial Hydrol.*, 3(2), 1-27.

Dunne, T., and R.D. Black (1970), Partial area contributions to storm runoff in a small New England watershed, *Water Resour. Res.*, 6(5), 1296-1311.

Erskine, R.H., T.R. Green, J.A. Ramirez, and L.H. MacDonald (2006), Comparison of grid-based algorithms for computing upslope contributing area, *Water Resour. Res.*, 42, 1-9.

Florinsky, I.V. (1998), Combined analysis of digital terrain models and remotely sensed data in landscape investigations, *Prog. in Phys. Geography*, 22(1), 33-60.

Gao, J., 1997. Resolution and accuracy of terrain representation by grid DEMs at a micro-scale, *International Journal of Geographical Information Science*, 11(2), 199-212.

Garbrecht, J., and L.W. Martz (2000), Digital elevation model issues in water resources modeling. In *Hydrologic and Hydraulic Modeling Support with Geographic Information Systems*, D. Maidment and D. Djokic (Eds), pp. 1-27 (Redland, CA: ESRI Press).

Gilbert, J.M., and B. Locke (2007), Restoring Rondeau Bay's Ecological Integrity. The Lake Erie Management Unit, Ontario Ministry of Natural Resources, Burlington ON: pp 40.

Grimaldi, S., F. Nardi, F. Di Benedetto, E. Istanbulluoglu, and R.L. Bras (2007), A physically-based method for removing pits in digital elevation models, *Advanc. in Water Resour.*, 30, 2151-2158.

Hutchinson, M.F. (1989), A new procedure for gridding elevation data and stream line data with automatic removal of spurious pits, *J. Hydrol.*, 106, 211-232.

Jenson, S.K. (1991), Applications of hydrologic information automatically extracted from digital elevation models, *Hydrol. Process.* 5, 31-44.

Jenson, S.K., and J.O. Domingue (1988), Extracting topographic structure from digital elevation data for geographical information system analysis, *Photogramm. Engin. and Remote Sens.*, 54(1), 1593-1600.

Kienzle, S (2004), The effect of DEM raster resolution on first order, second order and compound terrain derivatives, *Transactions in GIS*, 8(1), 83-111.

Lindsay, J.B., 2016a. Efficient hybrid breaching-filling sink removal methods for flow path enforcement in digital elevation models, *Hydrological Processes*, 30(6), 846–857. DOI: 10.1002/hyp.10648

Lindsay, J.B., 2016b. The practice of DEM stream burning revisited, *Earth Surface Processes and Landforms*, 41(5), 658–668. DOI: 10.1002/esp.3888

Lindsay, J.B., 2014. The Whitebox Geospatial Analysis Tools project and open-access GIS. Proceedings of the GIS Research UK 22nd Annual Conference, The University of Glasgow, 16-18 April, DOI: 10.13140/RG.2.1.1010.8962.

Lindsay, J.B., and I.F. Creed (2006), Distinguishing actual and artifact depressions in digital elevation data, *Comput. and Geosci.*, 32, 1192-1204.

Lindsay, J.B., and I.F Creed (2005), Removal of artifact depressions from digital elevation models: towards a minimum impact approach, *Comput. and Geosci.*, 19: 3113-3126.

Lindsay, J.B. and K. Dhun (2015), Modelling surface drainage patterns in altered landscapes using LiDAR, *Int. J. of Geog. Inf. Sci.,* 29(3): 397-411.

Liu, Y.B., S. Gebremeskel, F. Dem Smedt, L. Hoffman, and L. Pfister (2003), A diffusive transport approach for flow routing in GIS-based flood modeling, *J. Hydrol.*, 283, 91-106.

Martz, L.W., and J. Garbrecht (1999), An outlet breaching algorithm for the treatment of closed depressions in a raster DEM, *Comp. & Geoscie.* 25, 835-844.

Martz, L.W., and J. Garbrecht (1998), The treatment of flat areas and depressions in automated drainage analysis of raster digital elevation models, *Hydrol. Processes*, 12, 843-855.

Molder, B., Cockburn, J., Berg, A., Lindsay, J., & Woodrow, K. (2015). Sediment-assisted nutrient transfer from a small, no-till, tile drained watershed in Southwestern Ontario, Canada. *Agricultural Water Management*, *152*, 31-40.

Norcliffe, G.B. (1982), *Inferential Statistics for Geographers*. The Anchor Press Ltd: United Kingdom, 272 pp.

O'Callaghan, J.F., and D.M. Mark (1984), The extraction of drainage networks from digital elevation data, *Comput. Vision, Graphics, and Image Process.*, 28, 323-344.

Planchon, O., and F. Darboux (2001), A fast, simple and versatile algorithm to fill the depressions of digital elevation models, *Catena*, 46, 159-176.

Quinn, P., K. Beven, P. Chevallier, and O. Planchon (1991), The prediction of hillslope flow paths for distributed hydrological modeling using digital terrain models, *Hydrol. Processes*, 5, 59-59.

Rieger, W. (1998), A phenomenon-based approach to upslope contributing area and depressions in DEMs, *Hydrol. Processes*, 12, 857-872.

Robinson, G.J. (1994), The accuracy of digital elevation models derived from digitized contour data, *Photogramm. Rec.*, 14(83), 805-814.

Saulnier, G., C. Obled, and K. Beven (1997), Analytical compensation between DTM grid resolution and effective values of saturated hydraulic conductivity within the TOPMODEL framework, *Hydrol. Processes*, 11, 1331-1346.

Saunders, W. (1999) Preparation of DEMs for use in environmental modeling analysis. In *ESRI User Conference*, pp. 24-30.

Sørensen, R. and J. Seibert, 2007. Effects of DEM resolution on the calculation of topographical indices: TWI and its components, *Journal of Hydrology*, 347(1),79-89.

Tarboton, D.G. (1997), A new method for the determination of flow directions and upslope areas in grid digital elevation models, *Water Resour. Res.*, 33(2), 309-319.

Tarboton, D.G., R.L. Bras, and I. Rodigues-Iturbe (1991), On the extraction of channel networks from digital elevation data, *Hydrol. Processes*, 5, 81-100.

Tribe, A. (1992), Automated recognition of valley lines and drainage networks from grid digital elevation models: a review and a new method, *J. Hydrol.*, 139, 263-293.

Walker, J.P., and G.R. Willgoose (1999), On the effect of digital elevation model accuracy on hydrology and geomorphology, *Water Resour. Res.,* 35(7), 2259-2268.

Wang, L., and H. Liu (2006), An efficient method of identifying and filling surface depressions in digital elevation models for hydrologic analysis and modelling, *Internat. J. Geo. Informat. Science*, 20(2), 193-213.

Wolock, D.M. and G.J. McCabe, 2000. Differences in topographic characteristics computed from 100- and 1000-m resolution digital elevation model data, *Hydrological processes*, 14(6), 987-1002.

Wolock, D.M., and C.V. Price (1994), Effects of digital elevation model map scale and data resolution on a topography based watershed model, *Water Resour. Res.*, 30, 3041-3052.

Wu, S., Li, J. and G.H. Huang, 2008. A study on DEM-derived primary topographic attributes for hydrologic applications: Sensitivity to elevation data resolution, *Applied Geography*, 28(3), 210-223.

Zhang, J.X., K. Chang, and J.Q. Wu (2008), Effects of DEM resolution and source on soil erosion modelling: a case study using the WEPP model, *Intern. J. Geograph. Info. Scien.*, 22(8), 925-942.

Zhang, W., and D.R. Montgomery (1994), Digital elevation model grid size, landscape representation, and hydrologic simulations, *Water Resour. Res.*, 30(4), 1019-1028.